Structure and Properties of a New Family of Nearly Equiatomic Rare-Earth Metal-Tin-Germanides $RESn_{1+x}Ge_{1-x}$ (RE = Y, Gd−Tm): an Unusual Example of Site Preferences Between Elements from the Same Group

Paul H. Tobash,[†] John J. Meyers,[†] Gary DiFilippo,[†] Svilen Bobev,*[,†] Filip Ronning,[‡] Joe D. Thompson,[‡] and John L. Sarrao[‡]

Department of Chemistry and Biochemistry, University of Delaware, Newark, Delaware 19716, and Materials Physics and Applications Division, Los Alamos National Laboratory, Los Alamos, New Mexico 87545

Received November 28, 2007. Revised Manuscript Received January 9, 2008

Seven nearly stoichiometric compounds with general formulas $RESn_{1+x}Ge_{1-x}$ (RE = Y, Gd−Tm; $x \approx \pm 0.15$) have been synthesized from the corresponding elements using high-temperature reactions and molten Sn as a metal flux. They crystallize with the centrosymmetric space group *Cmcm* (No. 63) and their structures can be viewed as built up of two distinct polyanionic moieties: infinite $^{1}_{\infty}[Ge_2]$ zigzag chains and square sheets of tin atoms, $^{2}_{\infty}[Sn]$, with rare-earth cations enclosed between them. Within this formalism, such a bonding arrangement can also be described as a ternary derivative of the $ZrSi_2$ structure (Pearson's symbol *oC*12), obtained by "coloring" the anionic sites with two different elements, Ge and Sn in the present case. This is a unique aspect of the crystal chemistry of the intermetallic compounds in general, because elements from the same group typically do not show a tendency for site preferences. It is discussed in detail, along with an analysis of the trends across the whole series. The temperature dependence of the magnetic susceptibility, resistivity, and specific heat for all members of this family (some measured down to 400 mK and in applied fields up to 70 kOe) are reported as well. All lanthanide compounds are metallic and order antiferromagnetically at low temperatures.

Introduction

Intermetallic compounds formed between the rare-earth or alkaline-earth metals in combination with the early to-mid *p*-block elements offer a multitude of bonding interactions.[1–8] Their rich chemistry has already been at the focus of many experimental and theoretical investigations.[1–11] Two extremes can be specifically mentioned - "electron-excessive"[3] and "electron-deficient"[7] systems, leading to a variety of unprecedented hypoelectronic or hyperelectronic bonding arrangements in structures featuring discrete metal clusters,[1,2] infinite chains and layers,[3–5] or extended 3D networks.[6–9] Recently, the interest in such materials has shifted toward the prospects for rational structure-alteration by substitution

* Corresponding author. Phone: (302) 831-8720. Fax: (302) 831-6335. E-mail: bobev@udel.edu.
[†] University of Delaware.
[‡] Los Alamos National Laboratory.

(1) Kauzlarich, S. M. In *Chemistry, Structure and Bonding of Zintl Phases and Ions*; Kauzlarich, S. M., Ed.; VCH Publishers: New York, 1996; and references therein.
(2) (a) Zhao, J.-T.; Corbett, J. D. *Inorg. Chem.* **1995**, *34*, 378. (b) Chan, J. Y.; Wang, M. E.; Rehr, A.; Webb, D. J.; Kauzlarich, S. M. *Chem. Mater.* **1997**, *9*, 2131. (c) Zurcher, F.; Nesper, R. *Angew. Chem., Int. Ed.* **1998**, *37*, 3314. (d) Xu, Z.; Guloy, A. M. *J. Am. Chem. Soc.* **1998**, *120*, 7349. (e) Bobev, S.; Fritsch, V.; Thompson, J. D.; Sarrao, J. L.; Eck., B.; Dronskowski, R.; Kauzlarich, S. M. *J. Solid State Chem.* **2005**, *178*, 1071. (f) Ponou, S.; Fässler, T. F.; Tobías, G.; Canadell, E.; Cho, A.; Sevov, S. C. *Chem.—Eur. J.* **2004**, *10*, 3615. (g) Xia, S.-Q.; Hullmann, J.; Bobev, S.; Ozbay, A.; Nowak, E. R. *J. Solid State Chem.* **2007**, *180*, 2088.
(3) (a) Reviews: Papoian, G. A.; Hoffmann, R. *Angew. Chem., Int. Ed.* **2000**, *39*, 2409. (b) Mills, A. M.; Lam, R.; Ferguson, M. J.; Deakin, L.; Mar, A. *Coord. Chem. Rev.* **2002**, *233*, 207 and the references therein.
(4) (a) Xu, Z.; Guloy, A. M. *J. Am. Chem. Soc.* **1997**, *119*, 10541. (b) Mills, A. M.; Mar, A. *Inorg. Chem.* **2000**, *39*, 4599. (c) Salvador, J. R.; Bilc, D.; Mahanti, S. D.; Hogan, T.; Guo, F.; Kanatzidis, M. G. *J. Am. Chem. Soc.* **2004**, *126*, 4474. (d) Xie, Q.; Nesper, R. *Z. Anorg. Allg. Chem.* **2006**, *632*, 1743.
(5) (a) Mao, J.-G.; Xy, Z.; Guloy, A. M. *Inorg. Chem.* **2001**, *40*, 4472. (b) Mills, A. M.; Mar, A. *J. Am. Chem. Soc.* **2001**, *123*, 1151. (c) Ponou, S.; Fässler, T. F. *Inorg. Chem.* **2004**, *43*, 6124.
(6) (a) Bryan, J. D.; Stucky, G. D. *Chem. Mater.* **2001**, *13*, 253. (b) Seo, D.-K.; Corbett, J. D. *J. Am. Chem. Soc.* **2001**, *123*, 4512. (c) Kim, S.-J.; Kanatzidis, M. G. *Inorg. Chem.* **2001**, *40*, 3781. (d) Mao, J.-G.; Goodey, J.; Guloy, A. M. *Inorg. Chem.* **2002**, *41*, 931. (e) Jiang, J.; Kauzlarich, S. M. *Chem. Mater.* **2006**, *18*, 435.
(7) (a) Haussermann, U.; Amerioun, S.; Eriksson, L.; Lee, C. S.; Miller, G. J. *J. Am. Chem. Soc.* **2002**, *124*, 4371. (b) Tkachuk, A. V.; Mar, A. *J. Solid State Chem.* **2007**, *180*, 2298. (c) Li, B.; Corbett, J. D. *Inorg. Chem.* **2007**, *46*, 2237.
(8) (a) Alemany, P.; Llunell, M.; Canadell, E. *Inorg. Chem.* **2006**, *45*, 7235. (b) Seo, D.-K.; Corbett, J. D. *J. Am. Chem. Soc.* **2000**, *122*, 9621.
(9) (a) Papoian, G. A.; Hoffmann, R. *J. Am. Chem. Soc.* **2001**, *123*, 6600. (b) Munzarova, M. L.; Hoffmann, R. *J. Am. Chem. Soc.* **2002**, *124*, 4787.
(10) (a) Lam, R.; McDonald, R.; Mar, A. *Inorg. Chem.* **2001**, *40*, 952. (b) Mozharivskyj, Y.; Choe, W.; Pecharsky, A. O.; Miller, G. J. *J. Am. Chem. Soc.* **2003**, *125*, 15183. (c) You, T.-S.; Grin, Y.; Miller, G. J. *Inorg. Chem.* **2007**, *46*, 8801.
(11) (a) Nordell, K. J.; Miller, G. J. *Inorg. Chem.* **1999**, *38*, 579. (b) Häussermann, U.; Svensson, C.; Lidin, S. *J. Am. Chem. Soc.* **1998**, *120*, 3867. (c) Ganguli, A. K.; Corbett, J. D.; Köckerling, M. *J. Am. Chem. Soc.* **1998**, *120*, 1223. (d) Corbett, J. D. *Angew. Chem., Int. Ed.* **2000**, *39*, 670. (e) Wu, L.-M.; Kim, S.; Seo, D.-K. *J. Am. Chem. Soc.* **2005**, *127*, 15682. (f) Tobash, P. H.; Bobev, S. *J. Am. Chem. Soc.* **2006**, *128*, 3532.

10.1021/cm7033799 CCC: $40.75
Published on Web 02/27/2008

or addition of electron-poorer or electron-richer main-group elements.[10] Lateral studies aimed at tuning the valence electron concentration by analogous changeover of cations from the same or different groups in the periodic table have probed the limits of both the geometric and electronic ranges of stability in many types of structures.[11]

Intrigued by the idea of how such simple approaches can yield a wealth of structural novelties and properties, we focused our attention on extending our earlier studies on the family of ternary compounds RE_2InGe_2 (RE = Sm, Gd−Ho, Yb)[12] in a direction toward the electron-richer Sn. The two main reasons that motivated this work are simple: (1) the most intriguing aspect of the RE_2InGe_2 structure is that it contains an In atom in square-planar geometry, which is suggested to be in a zero-oxidation state by recent computational studies (i.e., the electronic configuration is $[Kr]5s^25p^1$).[13] This argument is also supported by the fact that the stability range of this structure extends well beyond group 13, to groups 12, 11, and even to the early members of group 2, which pointed toward the possibility of unparalleled electronic properties had the Sn-analogs been able to exist. (2) The ease of synthesis of RE_2InGe_2 (RE = Sm, Gd−Yb) employing the metal-flux technique[14] and the prospect of using Sn in place of In, seemed to be a reasonable working hypothesis as well. Instead, the efforts to substitute Sn for In proved unsuccessful and afforded the new family of nearly equiatomic ternary compounds $RESn_{1+x}Ge_{1-x}$ (RE = Y, Gd−Tm; $x \approx \pm 0.15$). With this paper, we report the structures and the physical properties of these new ternary phases, which for the sake of simplicity, are referred to as RESnGe hereafter (RE = rare-earth metal). Detailed discussions on the structure and bonding in this series are given for one member of the family, $TmSn_{1.02(1)}Ge_{0.98(1)}$ (i.e., TmSnGe). Among the seven compounds, TmSnGe was chosen as an example because its binary analog $TmGe_2$, previously recognized only from its powder X-ray diffraction pattern,[15,16] was also synthesized in a single-crystalline form. This made possible the careful side-by-side comparison between the two structures, both of which were unequivocally elucidated by single-crystal X-ray diffraction. In addition, short analyses of the structural trends across the series, as well as a comprehensive overview of the properties, are discussed in a broader context.

Experimental Section

Synthesis. All manipulations were performed inside an argon-filled glovebox with controlled oxygen and moisture levels below 1 ppm or under vacuum. The metals were purchased from Alfa or Ames Laboratory (>99.9%) and were used as received. The reactions were carried out in 2 cm^3 alumina crucibles, which were subsequently encapsulated in fused silica ampoules and flame-sealed under vacuum. In a typical experiment, a reaction mixture containing the starting materials in a molar ratio RE:Ge:Sn = 1:1:10 was heated to 1373 K (300°/h), equilibrated at this temperature for 1.5 h, and subsequently cooled to 773 K (30°/h). $TmGe_2$ was synthesized following the same approach but using In flux instead. At this temperature, the excess molten flux (Sn, mp 505 K; or In, mp 430 K) was easily removed and the grown crystals were isolated. Further details on the general experimental procedures, techniques and temperature profiles used in the syntheses of the remaining isostructural compounds are listed in the Supporting Information.

Table 1. Selected Single-Crystal Data Collection and Refinement Parameters for TmSnGe and $TmGe_2$

empirical formula	$TmSn_{1.02(2)}Ge_{0.98(2)}$	$TmGe_2$
fw	361.13	314.11
radiation type, wavelength	Mo Kα, 0.71073 Å	
temperature	120 K	
space group	*Cmcm* (No. 63)	
unit cell dimensions (Å)	$a = 4.2022(13)$	$a = 3.9970(7)$
	$b = 15.935(5)$	$b = 15.719(3)$
	$c = 4.0247(12)$	$c = 3.8604(7)$
unit cell volume, $Z = 4$	269.50(14) $Å^3$	242.54(8) $Å^3$
ρ_{calcd} (g cm^{-3})	8.900	8.602
absorption coefficient (mm^{-1})	52.489	60.461
cryst size (mm^3)	0.07 × 0.04 × 0.04	0.05 × 0.03 × 0.02
extinction coefficient	0.0024(3)	0.0018(3)
GOF on F^2	1.374	1.253
data/params	182/16	182/14
R_1/wR_2 ($I > 2\sigma(I)$)[a]	$R_1 = 0.0173$	$R_1 = 0.0185$
	$wR_2 = 0.0418$	$wR_2 = 0.0415$
R_1/wR_2 (all data)[a]	$R_1 = 0.0175$	$R_1 = 0.0191$
	$wR_2 = 0.0419$	$wR_2 = 0.0416$
largest diff. peak/hole (e $Å^{-3}$)	0.967/−1.856	0.812/−0.977

[a] $R_1 = \Sigma||F_o| - |F_c||/|F_o|$; $wR_2 = [\Sigma[w(F_o^2 - F_c^2)^2]/\Sigma[w(F_o^2)^2]]^{1/2}$, and $w = 1/[\sigma^2F_o^2 + (AP)^2 + BP]$, $P = (F_o^2 + 2F_c^2)/3$; A and B are weight coefficients.

Powder X-ray Diffraction. X-ray powder diffraction patterns were taken at room temperature on a Rigaku MiniFlex powder diffractometer using Cu Kα radiation. Typical runs included $\theta-\theta$ scans ($2\theta_{max} = 80°$) with scan steps of 0.05° and 5 s/step counting time. The JADE 6.5 software package was used for data analysis. The intensities and the positions of the experimentally observed peaks and those calculated from the crystal structures matched very well. The recorded powder patterns for the seven samples are provided as Supporting Information (Figure S1 and S2); the least-squares refined unit cell parameters (using Si as an internal standard) are given in Table S1 in the Supporting Information.

Single-Crystal X-ray Diffraction. Only a brief description on the data collection for TmSnGe and $TmGe_2$ is provided herein; analogous information for the remaining six RESnGe compounds is summarized in Tables S2 and S3 in the Supporting Information.

A full sphere of reciprocal-space data were collected at 120 K on a Bruker SMART CCD-based diffractometer. The crystals of TmSnGe and $TmGe_2$ were chosen from the corresponding flux reactions and cut to suitable dimensions for data collection (ca. 0.05 mm^3). They were mounted on glass fibers using Paratone N oil. The data collections were carried out in batch runs at different ω and φ angles. Frame width was 0.5° in ω and θ with data acquisition time of 8 s/frame. SMART and SAINT were used for the data acquisition and data integration, respectively. The unit cell parameters were refined using all measured reflections. Semiempirical absorption correction based on equivalents was applied using SADABS. The structure solution (direct methods) and structure refinement (full matrix least-squares on F^2) were done using the SHELXTL package. Further details of the data collection and structure refinements parameters are given in Table 1, whereas the structure refinements parameters for the remaining six compounds

(12) Tobash, P. H.; Lins, D.; Bobev, S.; Lima, A.; Hundley, M. F.; Thompson, J. D.; Sarrao, J. L. *Chem. Mater.* **2005**, *17*, 5567.
(13) Whangbo, M.-H.; Lee, C.; Köhler, J. *Angew. Chem., Int. Ed.* **2006**, *45*, 7465.
(14) (a) Canfield, P. C.; Fisk, Z. *Philos. Mag. B* **1992**, *65*, 1117. (b) Kanatzidis, M. G.; Pöttgen, R.; Jeitschko, W. *Angew. Chem., Int. Ed.* **2005**, *44*, 6996.
(15) Villars, P.; Calvert, L. D. *Pearson's Handbook of Crystallographic Data for Intermetallic Phases*, 2nd ed.; American Society for Metals: Materials Park, OH, 1991.
(16) Eremenko, V. N.; Meleshevich, K. A.; Buyanov, Y. I.; Martsenyuk, P. S. *Porosh. Metal.* **1989**, *28*, 543.

are summarized in Table 2. Atomic coordinates, equivalent isotropic displacement parameters, and important bond distances for TmSnGe and $TmGe_2$ are given in Tables 3 and 4. The combined crystallographic information file (CIF) is provided as Supporting Information.[17]

Physical Property Measurements. All herein discussed physical property measurements were carried out on the very same crystals (or pieces from the same crystal), including the elemental analysis. For the resistivity measurements, in order to provide a clean surface for the measurements and to eliminate errors due to small amounts of residual Sn, the crystals were sand-paper polished.

Magnetic Susceptibility Measurements. Field-cooled dc magnetization (M) measurements were performed for all compounds using a Quantum Design MPMS2 SQUID magnetometer. The measurements were done with crystals aligned both perpendicular and parallel to the direction of the applied magnetic field ($H = 500$ Oe) in the temperature interval 5–290 K. In the case of ErSnGe, measurements were taken down to 2 K. The raw magnetization data were corrected for the holder contribution and converted to molar susceptibility ($\chi_m = M/H$).

Specific Heat and Resistivity Measurements. The specific heat data were measured in a He^4 cryostat using the thermal relaxation method within the temperature range 2−100 K. In the case of TmSnGe, specific heat measurements were done in a He^3 cryostat using the same method but within the temperature range of 0.4−5 K. The resistance was measured using the four-probe technique from 2 to 300 K with an excitation current of 1 mA. Since the crystals were large plates (typically 5–8 mm^2), the contacts were made by spot welding 0.001 in. platinum wires to their smooth surface. All measurements were taken along the direction of the plates (presumed to be perpendicular to the longest cell axis, the *b* axis). As stated before, to minimize the geometric errors, all crystals were polished to roughly 200 μm in thickness.

Elemental Analysis. Single crystals were mounted on to carbon tape and placed in a Jeol 7400 F electron microscope equipped with an INCA-Oxford energy-dispersive spectrometer. The microscope was operated at 10 μA beam current at 15 kV accelerating potential. Data were acquired for several spots on the same crystal and averaged. The analysis gave ratios (at %) of RE:Sn:Ge ≈ 1:1:1. Normalization per rare-earth metal yielded slightly "Sn-rich" compositions, in good agreement with the refinements from single-crystal diffraction data (Tables 1 and 2). Because polished crystals were used in each measurement, residual tin on the surface, which could have biased the analyses can be ruled out.

Results

Synthesis. All RESnGe compounds (RE = Y, Gd−Tm) can be readily synthesized from reactions in Sn flux in high yields and as a single-phase product (large plates). The only other phase present according to the powder patterns was elemental Sn (Figure S1). Attempts to extend the series to include EuSnGe and YbSnGe failed - these reactions produced the binary cubic phases $EuSn_3$ and $YbSn_3$.[15] Similar was the outcome of the reactions with the early rare-earth metals La, Ce and Pr. In the case of Nd and Sm, aside from the recurring $NdSn_3$ and $SmSn_3$ phases,[15] other, presumably new ternary compounds were formed, but their structures

(17) CIFs have also been deposited with Fachinformationszentrum Karlsruhe, 76344 Eggenstein-Leopoldshafen, Germany (fax: (49) 7247–808–666; e-mail: crysdata@fiz.karlsruhe.de), depository numbers CSD-418788 (GdSnGe); CSD-418789 (TbSnGe); CSD-418790 (DySnGe); CSD-418791 (HoSnGe); CSD-418792 (ErSnGe); CSD-418793 (TmSnGe); CSD-418794 (YSnGe); CSD-418795 ($TmGe_2$).

Table 2. Selected Single-Crystal Data Collection and Refinement Parameters for RESnGe (RE = Y, Gd−Er)

empirical formula	$YSn_{1.14}Ge_{0.86(2)}$	$GdSn_{1.17}Ge_{0.83(2)}$	$TbSn_{1.12}Ge_{0.88(2)}$	$DySn_{1.09}Ge_{0.91(2)}$	$HoSn_{1.10}Ge_{0.90(2)}$	$ErSn_{1.08}Ge_{0.92(2)}$
fw	286.76	356.37	356.34	357.93	360.59	362.34
radiation type, wavelength			Mo Kα, 0.71073 Å			
temperature			120 K			
space group			*Cmcm* (No. 63)			
unit cell dimensions (Å)	$a = 4.2511(14)$	$a = 4.3005(9)$	$a = 4.266(2)$	$a = 4.251(2)$	$a = 4.247(2)$	$a = 4.209(3)$
	$b = 16.296(5)$	$b = 16.441(4)$	$b = 16.293(6)$	$b = 16.197(8)$	$b = 16.127(7)$	$b = 16.006(10)$
	$c = 4.0633(13)$	$c = 4.0944(9)$	$c = 4.062(2)$	$c = 4.058(2)$	$c = 4.069(2)$	$c = 4.029(3)$
unit cell volume, $Z = 4$	281.5(2) Å^3	289.50(11) Å^3	282.4(2) Å^3	279.5(2) Å^3	278.7(2) Å^3	271.4(3) Å^3
ρ_{calcd} (g cm^{-3})	6.767	8.176	8.365	8.507	8.593	8.867
absorption coefficient (mm^{-1})	39.234	40.862	43.546	45.482	47.171	50.229
cryst size (mm^3)	$0.07 \times 0.04 \times 0.04$	$0.08 \times 0.04 \times 0.03$	$0.06 \times 0.05 \times 0.04$	$0.08 \times 0.06 \times 0.05$	$0.05 \times 0.04 \times 0.03$	$0.05 \times 0.04 \times 0.03$
extinction coefficient	n/a	0.0048(4)	0.0002(3)	0.0002(2)	0.0017(2)	0.0030(4)
GOF on F^2	1.209	1.277	1.037	1.124	1.044	1.159
data/params	187/15	188/16	189/16	186/16	187/16	184/16
R_1/wR_2 ($I > 2\sigma(I)$)[a]	$R_1 = 0.0204$	$R_1 = 0.0195$	$R_1 = 0.0298$	$R_1 = 0.0226$	$R_1 = 0.0159$	$R_1 = 0.0248$
	$wR_2 = 0.0475$	$wR_2 = 0.0471$	$wR_2 = 0.0734$	$wR_2 = 0.0519$	$wR_2 = 0.0335$	$wR_2 = 0.0548$
R_1/wR_2 (all data)	$R_1 = 0.0208$	$R_1 = 0.0204$	$R_1 = 0.0335$	$R_1 = 0.0260$	$R_1 = 0.0220$	$R_1 = 0.0259$
	$wR_2 = 0.0478$	$wR_2 = 0.0476$	$wR_2 = 0.0769$	$wR_2 = 0.0535$	$wR_2 = 0.0367$	$wR_2 = 0.0553$
largest diff. peak/hole (e Å^{-3})	2.397/−1.158	1.266/−1.757	2.696/−1.753	2.785/−1.353	0.851/−0.843	1.804/−1.189

[a] $R_1 = \Sigma||F_o| - |F_c||/\Sigma|F_o|$; $wR_2 = [\Sigma[w(F_o^2 - F_c^2)^2]/\Sigma[w(F_o^2)^2]]^{1/2}$, and $w = 1/[\sigma^2 F_o^2 + (AP)^2 + BP]$, $P = (F_o^2 + 2F_c^2)/3$; A and B are weight coefficients.

Table 3. Atomic Coordinates and Equivalent Isotropic Displacement Parameters (U_{eq}[a]) for TmSnGe and $TmGe_2$

atom	Wyckoff	*x*	*y*	*z*	U_{eq} (Å)^2
			TmSnGe		
Tm	4*c*	0	0.09627(3)	1/4	0.0093(3)
Sn[b]	4*c*	0	0.74638(5)	1/4	0.0092(4)
Ge[b]	4*c*	0	0.44322(8)	1/4	0.0105(5)
			$TmGe_2$		
Tm	4*c*	0	0.10358(3)	1/4	0.0090(3)
Ge1	4*c*	0	0.44727(8)	1/4	0.0102(3)
Ge2	4*c*	0	0.74730(8)	1/4	0.0116(3)

[a] U_{eq} is defined as one-third of the trace of the orthogonalized U_{ij} tensor. [b] The final refined Sn/Ge occupancies for all seven structures are provided as Supporting Information.

Table 4. Side-by-Side Comparison of Selected Bond Distances in TmSnGe and $TmGe_2$

atom pair		distance (Å)	atom pair		distance (Å)
		TmSnGe			
Tm	4 × Ge	2.9766(7)	Sn	4 × Sn	2.9116(6)
	2 × Ge	3.2191(12)			
	2 × Sn	3.1838(9)	Ge	2 × Ge	2.706(2)
	2 × Sn	3.2150(11)			
		$TmGe_2$			
Tm	4 × Ge1	2.8911(5)	Ge2	4 × Ge2	2.7797(4)
	2 × Ge2	3.0161(10)			
	2 × Ge2	3.0365(12)	Ge1	2 × Ge1	2.544(2)
	2 × Ge1	3.1671(11)			

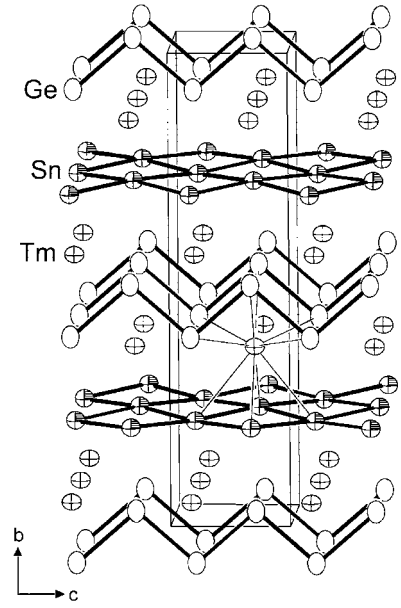

Figure 1. Projection of the crystal structure of TmSnGe, viewed approximately down the *a*-axis. Tm cations are shown with crossed ellipsoids, Ge in the zigzag chains are shown with boundary ellipses, and Sn in the square nets are drawn with full thermal ellipsoids. Probability level is 95% and the unit cell is outlined.

remain elusive and will be at the focus of future studies. Arc-melting stoichiometric amounts of the elements also affords the RESnGe phases for the mid-to-late rare-earth metals in good yields and gives mixtures of binary phases for the early rare-earth metals.

We also note that in all seven cases, as evident from the powder X-ray diffraction patterns, there was a dependence of the cell volume on the reaction conditions, suggesting a small phase width. There were no indications for phase segregation upon slight changes in the nominal compositions, from which it can be inferred that the homogeneity range (x) in $RESn_{1+x}Ge_{1-x}$ is not very large. On the basis of the unit-cell parameters for a large number of samples, we estimate that the deviations from the strictly equiatomic formulas cannot be larger than ca. 10–15 at %. However, to avoid "sample dependence" errors and to ensure reliability, crystals from the same batch were used for all physical property measurements.

According to the diffraction patterns, both the powders and the single crystals are stable in air for extended periods of time, greater than 6 months.

Structure Refinements. Formally, the atomic arrangement in the RESnGe structure is isomorphous with the $ZrSi_2$ type. This structure is centrosymmetric (space group *Cmcm* (No. 63), Pearson's symbol *oC*12)[15] with 3 crystallographically unique atoms in the asymmetric unit, all in special positions, and was used as a starting model in all seven refinements. In all instances, a clear and systematic trend was immediately evident; the site that corresponds to the atom forming the square sheets (Figure 1) refined as ca. 90–100% occupied by Sn, and with an occupancy much greater than unity when Ge was placed on this position. The occupancy refinement of the other site, the one that corresponds to the atom forming the zigzag chains (Figure 1) showed completely reversed leaning - it refined as nearly 100–110% occupied by Ge, and close to 60% occupied by Sn. This hinted at the possibility that Sn and Ge order in the structure, leading to an equiatomic formula RESnGe, a conclusion that is supported by the discussed EDX analyses, as well as bond distances and changes in the unit-cell parameters.

A further and more detailed account of the steps taken during the refinement cycles is provided in the Supporting Information. The structures of TmSnGe and $TmGe_2$ are discussed in parallel next.

Structure and Bonding. The structure of TmSnGe is shown in Figure 1. It is best described as being composed of two distinct polyanionic fragments stacked in the direction of the crystallographic *b*-axis, which are interspaced by Tm cations. These are the above-mentioned zigzag chains of Ge, and the square sheets of Sn. As a comparison, we refer to the isostructural $TmGe_2$ (Table 1), which has the same polyanionic subnetwork, made of Ge atoms only. Cation coordination is depicted and discussed briefly in Supporting Information. Detailed descriptions of the two fragments follow.

The Ge zigzag chains in both TmSnGe and $TmGe_2$ propagate along the direction of the crystallographic *c*-axis and can be recognized as having the same topology as those found in TmGe (CrB type).[15,16] These fragments of the structure are "intercalated" by the square nets, made of Sn in TmSnGe, and made of Ge in $TmGe_2$. A closer look at both fragments is given in Figure S3 (Supporting Information). The Ge-Ge distances within the $^1_\infty[Ge_2]$ zigzag chains in TmSnGe measure 2.706(2) Å (Table 4) and the corresponding Ge-Ge-Ge angles are 96.07(8)°. The distances and the angles in the isostructural RESnGe (RE = Y, Gd−Er) compounds are in the same range - between 2.70 and 2.74(1) Å and 96.3(1)–97.41(8)°, respectively. A careful examination of these structural parameters within the whole RESnGe

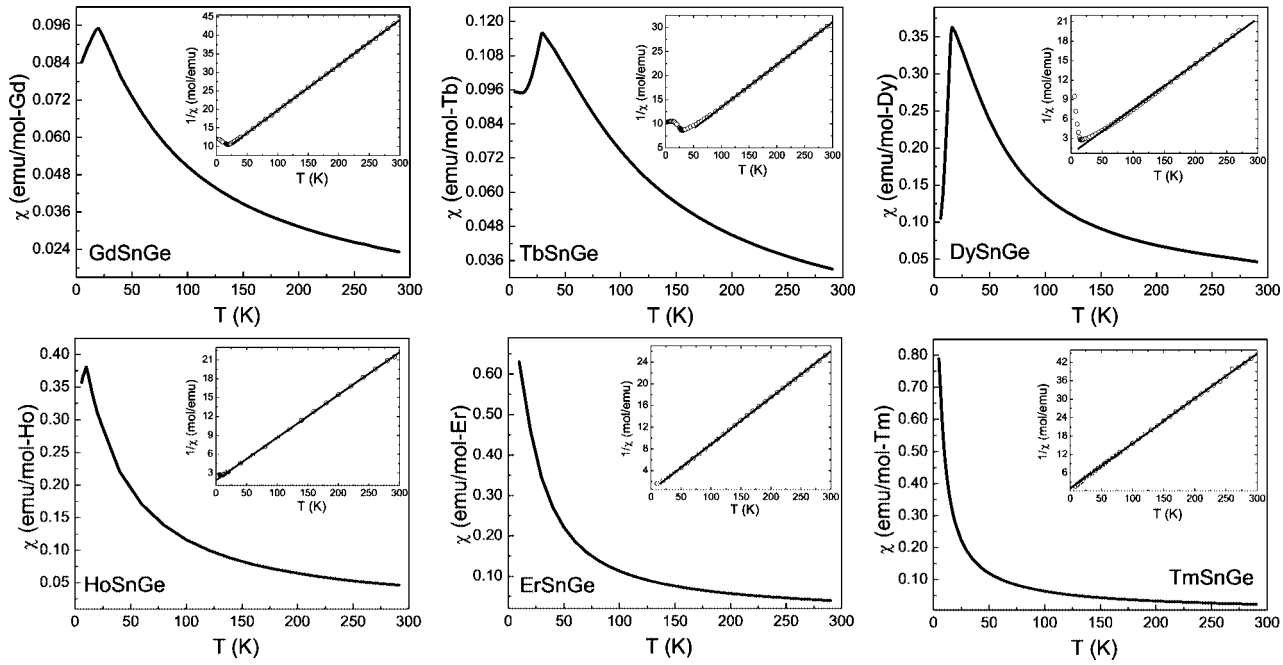

Figure 2. Temperature dependence of the magnetic susceptibility χ(T) for RESnGe (RE = Gd−Tm). The insets show the inverse magnetic susceptibility $\chi^{-1}(T)$ and the linear fits to the Curie–Weiss law.

series suggests that they are invariant of the nature of the rare-earth metal (a compiled list of all distances and angles is given in the Supporting Information).

The Ge-Ge distances within the $^1_\infty$[Ge_2] zigzag chains in TmSnGe are understandably longer than those in $TmGe_2$, 2.706(2) vs 2.544(2) Å, respectively. This elongation is due to (1) the expansion of the unit cell in TmSnGe compared to that of its binary counterpart (Table 1), and (2) to the small admixture with Sn on this crystallographic site (as shown by the single crystal refinements). Comparing the "pure" Ge−Ge distance in $TmGe_2$ with those reported for other binary alkaline-earth and rare-earth metal germanides such as TmGe,[16] $DyGe_3$,[18] Yb_5Ge_4,[19] $CaGe_2$,[20a] Sm_3Ge_5,[20b] Gd_3Ge_4,[20c] $EuGe_2$,[20d] indicates that the interactions within the Ge chains are normal, covalent-type bonds. The Ge−Ge−Ge angle within the $^1_\infty$[Ge_2] zigzag chains in $TmGe_2$ is 98.686(9)°; the corresponding angle in TmSnGe is 96.07(8)°. Both are slightly larger than the 93.7(2)° angle in the isomorphous chains in TmGe,[16] but slightly smaller than the 101.1(2)° angle in the analogous triangular fragments in Tm_3Ge_4.[20c]

The square nets in TmSnGe are made exclusively of Sn atoms and the Sn−Sn distances are 2.9116(6) Å (Table 4). These are longer than the Sn-Sn distances found in the semiconducting α-Sn (2.810 Å),[15] but shorter than those in the metallic allotrope β-Sn (3.06_{axial} and 3.175_{apical} Å).[15] Sn-Sn distances in the same range are reported for some binary stannides such as $RESn_2$ (3.01–3.18 Å; RE = Tb−Lu),[15] $SrSn_4$ (3.040–3.302 Å),[21a] or $NaSn_5$ (3.143 Å).[21b] As was the case with the zigzag chains, there is no systematic dependence of bond-distances and angles in the tin nets with the decreasing size of the rare-earth metal when moving across the family (Supporting Information).

The corresponding square nets in $TmGe_2$ are made of Ge atoms, with distances between them 2.7797(4) Å. Such Ge−Ge interactions are clearly longer than those expected for the typical covalent bonds, as those in the above-mentioned $^1_\infty$[Ge_2] chains for instance, and may signify Ge-Ge bonding of nonclassical nature, a point that will be discussed further on. Similarly long distances are rare but not without precedent: Ge−Ge contacts on the order of 2.9 Å are reported for $LuGe_2$,[22a] UGe_2,[22b23] and $LaGe_5$.[22c]

Lastly, there is another particular point with regard to the $^2_\infty$[Sn] sheets in TmSnGe and the $^2_\infty$[Ge] sheets in $TmGe_2$ that deserves a closer examination: the fact that these layers are not perfectly flat but rather slightly puckered. In the case of TmSnGe, the distortion from the ideal planar geometry is slightly more pronounced as the Sn atoms are located approximately 0.058 Å above and below the [040] plane with bond angles of 92.38(2)° and 87.44(2)°. Alternatively in

(18) Schobinger-Papamantellos, P.; de Mooij, D. B.; Buschow, K. H. J. *J. Alloys Compd.* **1992**, *183*, 181.
(19) (a) Pani, M.; Palenzona, A. *J. Alloys Comp.* **2003**, *360*, 151. (b) Ahn, K.; Tsokol, A. O.; Mozharivskyj, Yu.; Gschneidner, K. A., Jr.; Pecharsky, V. K. *Phys. Rev. B.* **2005**, *72*, 054404–1.
(20) (a) Tobash, P. H.; Bobev, S. *J. Solid State Chem.* **2007**, *180*, 1575. (b) Tobash, P. H.; Lins, D.; Bobev, S.; Hur, N.; Thompson, J. D.; Sarrao, J. L. *Inorg. Chem.* **2006**, *45*, 7286. (c) Tobash, P. H.; DiFilippo, G.; Bobev, S.; Hur, N.; Thompson, J. D.; Sarrao, J. L. *Inorg. Chem.* **2007**, *46*, 8690. (d) Bobev, S.; Bauer, E. D.; Thompson, J. D.; Sarrao, J. L.; Miller, G. J.; Eck, B.; Dronskowski, R. *J. Solid State Chem.* **2004**, *177*, 3545.
(21) (a) Hoffmann, S.; Fässler, T. F. *Inorg. Chem.* **2003**, *42*, 8748. (b) Fässler, T. F.; Kronseder, C. *Angew. Chem., Int. Ed.* **1998**, *37*, 1571.
(22) (a) Chung, Y. R.; Sung, H. H.; Lee, W. H. *Phys. Rev. B* **2004**, *70*, 052511. (b) Boulet, P.; Daodi, A.; Potel, M.; Noel, H.; Gross, G. M.; Andre, G.; Bouree, F. *J. Alloys Compd.* **1997**, *247*, 104. (c) Fukuoka, H.; Yamanaka, S. *Phys. Rev. Lett.* **2003**, *67*, 094501.
(23) Although these layers are dubbed "square nets" throughout the text, it must not be forgotten that this description is just an approximation. The puckering of the nets increases as the size of the rare-earth metal cation increases, i.e., from Tm to Gd. This also coincides with the increase of the Sn-content, i.e., enlarging the unit cell, thereby making the separation of the two effects impossible.

Table 5. Selected Physical Property Data for RESnGe (RE = Y, Gd−Tm)[a]

compd	magnetic behavior[b]	μ_{calcd} (μ_B)	μ_{eff} (μ_B)	θ_p (K)	T_N (K)	ρ_{298} ($\mu\Omega$ cm)	ρ_4 ($\mu\Omega$ cm)
YSnGe	Pauli PM					32	7
GdSnGe	AFM	7.94	8.05	−59	19	85	28
TbSnGe	AFM	9.72	9.47	−49	29	61	18
DySnGe	AFM	10.65	10.55	−3	16	32	7
HoSnGe	AFM	10.61	10.84	−27	10	38	10
ErSnGe	AFM	9.58	9.41	−2	4	31	5
TmSnGe	AFM	7.56	7.41	−8	0.9	37	8

[a] The expected effective moments are calculated according to $\mu_{calcd} = g_J\sqrt{J(J+1)}$.[24] The reported Néel temperatures (T_N) are determined from $d\chi(T)/dT$. [b] Pauli PM stands for Pauli paramagnetic; AFM denotes antiferromagnetic.

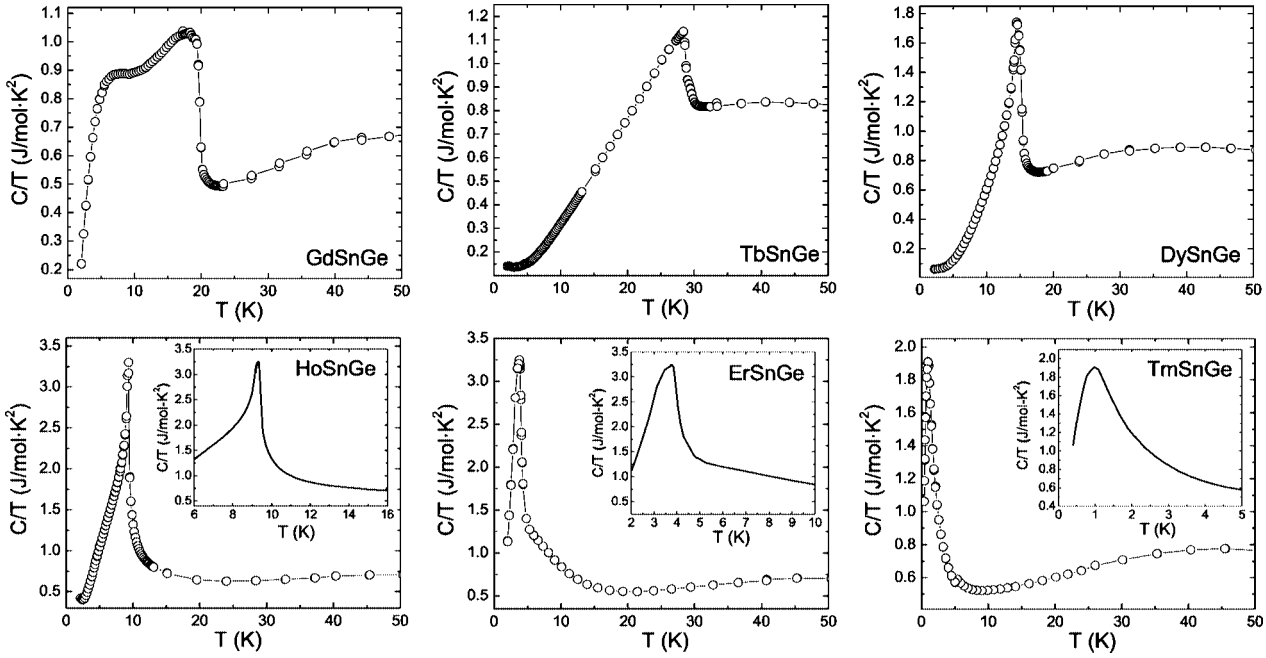

Figure 3. Temperature dependence of the specific heat for RESnGe (RE = Y, Gd−Tm). The data are represented in the form C_p/T vs T.

$TmGe_2$, the Ge atoms lie ca. 0.042 Å above and below the same plane with Ge−Ge−Ge angles of 91.94(2) and 87.96(2)°.

Properties. Plots of the temperature dependence of the magnetic susceptibility χ = M/H are shown in Figure 2. Above 30 K, all compounds exhibit paramagnetic behavior and $\chi(T)$ nicely follows the Curie–Weiss law $\chi(T) = C/(T - \theta_p)$,[24] where $C = N_A\mu_{eff}^2/3k_B$ is the Curie constant and θ_p is the Weiss temperature. At lower temperatures, the title compounds, with a possible exception of TmSnGe, order antiferromagnetically (Table 5) and the corresponding Néel temperatures (T_N) were determined from the midpoint of the jump in $d\chi/dT$. $TmGe_2$ also shows paramagnetic behavior and does not order down to 2 K (Figure S5 in the Supporting Information) YSnGe exhibits temperature-independent paramagnetism in the same temperature interval (see the Supporting Information, Figure S6). The experimentally determined effective magnetic moments are listed in Table 5 and are in very good agreement with the theoretically calculated values according to $\mu_{eff} = g_J\sqrt{J(J+1)}$.[24] θ_p values are negative as expected for antiferromagnetically ordered structures.

The results from the measurements of the specific heat are shown in Figure 3, plotted in the form C_P/T vs T. As can easily be seen from the figure, the temperature dependence of the specific heat provides additional evidence for the onset of the magnetic order for each of the RESnGe (RE = Gd−Tm) compounds and corroborates the ordering temperatures obtained from the magnetization measurements.

Resistivity measurements as a function of the temperature suggest that all RESnGe compounds are metallic, as evidenced from the presented plots in Figure 4. The room and low temperature resistivities are summarized in Table 5. Small kinklike features are visible in the data at the respective ordering temperatures, as shown in the insets of Figure 4. For all compounds, the dependence of the resistivity with the temperature follows a nearly linear behavior. At low temperatures, a slight concave ρ(T) dependence, according to $\rho(T) = \rho_0 + AT^2$,[24] can be observed for the last two members, ErSnGe and TmSnGe.

Discussion

The two main factors that determine the bonding in intermetallic phases are the sizes of the constituent atoms and the number of valence electrons (aka *vec* or valence electron concentration).[25] These principles have been formulated decades ago and have proven very effective in

(24) (a) Smart, J. S. *Effective Theories of Magnetism*; Saunders: Philadelphia, PA, 1966. (b) Kittel, C. *Introduction to Solid State Physics*, 7th ed.; John Wiley and Sons: Hoboken, NJ, 1996.

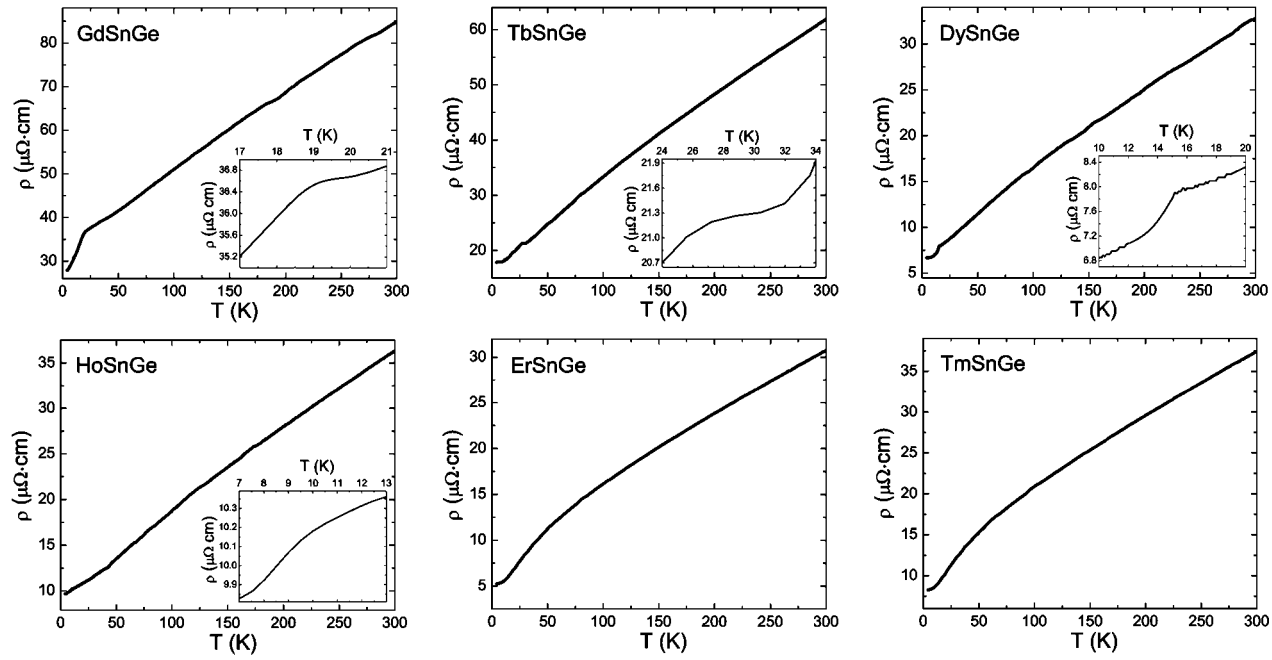

Figure 4. Four-probe electrical resistivity as a function of the temperature for RESnGe (RE = Y, Gd−Tm). Insets show magnified views at low temperatures.

rationalizing the structures of many simple compounds.[25] However, as the complexity of the structures increases, the analysis of the structure−bonding relationships becomes progressively more difficult and many issues remain unsettled. Of particular relevance to the discussion herein is the topic of how do different chemical elements arrange themselves within a given extended structure? This question is a part of the site preference problem in solids, often dubbed the "coloring" problem,[26] which requires a good estimation of the structural energy difference for different arrangements of atoms.

Within this formalism, the site selection will depend on the lowest energy, controlled by the extent of electron transfer and electron overlap.[26] Applying this approach to main-group homologues (different *p*-block elements, but from the same group in the periodic table), will not be straightforward because the "coloring effect" will likely be small. The main difficulty here clearly arises from the fact that the electronic requirements within the same group are unchanged, and the changes in the overlap (excluding the relativistic effects) due to the packing of atoms with different radii and slightly different electronegativities may not be sufficient to yield a preferred bonding pattern.[26] Indeed, a survey of the literature shows many examples, such as $Nb_5(Ge_xSn_{1-x})_2$,[27a] $Ba_6(Sn_xGe_{1-x})_{25}$,[27b] and $Ca(Sn_xGe_{1-x})_2$,[27c] among others, where a purely statistical distribution is reported. This is markedly different from the rare cases Ba_2BiSb_2,[5c] $K_2Bi_{8-x}Sb_xSe_{13}$,[28] $GdCuAs_{1+x}P_{1-x}$,[29] or $Gd_5Si_2Ge_2$,[30] where site preferences are observed.

Given these difficulties, how can one rationalize the RESnGe structure and more importantly, the Sn−Ge tendency to order within it? To begin, we would first like to bring attention to the pattern, followed by the binary compounds of the rare-earth metals and the group 14 elements Si, Ge, and Sn in a 1:2 stoichiometric ratio. With a few exceptions, they can be separated into three major structure types: AlB_2, α-$ThSi_2$, and $ZrSi_2$.[15] Recent case studies on these classes of compounds demonstrate that the preferred formation of one structure vs another is governed largely by the sizes (atomic radii) of the constituent elements.[3a] For instance, the α-$ThSi_2$ structure is prevailing for the silicides and germanides of the early to-mid rare-earth metals, whereas the AlB_2 type is dominant for the silicides and germanides of the mid-to-late rare-earth metals. $TmGe_2$ and $LuGe_2$ are the only digermanides with the $ZrSi_2$ type,[15] but there are not any disilicides of the rare-earth metals with this structure. On the other hand, all known $RESn_2$ compounds (RE = Gd−Tm) crystallize with the $ZrSi_2$ type structure.

Based on this information, one might conclude that the RESnGe compounds are just solid solutions of $REGe_2$ and $RESn_2$. However, the notion that $REGe_2$ and $RESn_2$ are the end members and that the RESnGe phases are simply solid solutions cannot explain why when Ge and Sn coexist in this arrangement, each element "prefers" either the zigzag chains or the almost planar sheets, respectively. Such a site-specific substitution of Sn for Ge can be related to the fact that the square-planar coordination is atypical for the early group 14

(25) Nesper, R *Angew. Chem., Int. Ed.* **1991**, *30*, 789, and references therein.
(26) Miller, G. J. *Eur. J. Inorg. Chem.* **1998**, 523.
(27) (a) Tanaka, M.; Horiuchi, H.; Shishido, T.; Fukuda, T. *Acta Crystallogr., Sect. C* **1993**, *49*, 437. (b) Kim, S.-J.; Hu, S.; Uher, C.; Hogan, T.; Huang, B.; Corbett, J. D.; Kanatzidis, M. G. *J. Solid State Chem.* **2000**, *153*, 321. (c) Ganguli, A. K.; Corbett, J. D. *J. Solid State Chem.* **1993**, *107*, 480.
(28) Kyratsi, T.; Chung, D. Y.; Kanatzidis, M. G. *J. Alloys Compd.* **2002**, *338*, 36.
(29) Mozharivskyj, Y.; Kaczorowski, D.; Franzen, H. F. *J. Solid State Chem.* **2000**, *155*, 259.
(30) Choe, W.; Miller, G. J.; Meyers, J.; Chumbley, S.; Pecharsky, A. O. *Chem. Mater.* **2003**, *15*, 1413.
(31) (a) Burdett, J. K.; Lee, S. *J. Am. Chem. Soc.* **1983**, *105*, 1079. (b) Tremel, W.; Hoffmann, R. *J. Am. Chem. Soc.* **1987**, *109*, 124. (c) Seo, D.-K.; Hoffmann, R *J. Solid State Chem.* **1999**, *147*, 26.

elements C and Si due to the strong s−p hybridization, but as the principle quantum number increases and the valence orbitals become more diffuse when moving down the group, square geometry becomes more feasible.[31]

This brings the idea of hypervalent bonding into the picture.[32] As carefully detailed by others,[3,9] the optimal number of electrons for zigzag chains of the *p*-block elements is suggested to be 6 e^-/atom, in analogy with the electron count in sulfur chains for instance.[3a] Considering the possibility for π-bonding within the chains, in analogy with polyacetylene, will give rise to a different overall bonding picture requiring 5 e^-/atom.[3a] Intermediate number of valence electrons (between 5 and 6 e^-/atom) can also result in stable configurations provided some interchain interactions exist. Using the fragment-orbital approach, the planar 4-connected nets can be rationalized as being the result of the linkage of zigzag chains.[31] The electron count in such networks obviously will not follow the classic octet rule, and must be explained by the idea of hypervalency: many theoretical treatments of such 2D-square lattices show the "preferred" electron count to be 6 e^-/atom.[31] These nuances in the bonding of chains vs layers are particularly well illustrated for the heavy pnicogens Sb and Bi.[3,9,31]

Returning to RESnGe, assigning formal charges to the Ge atoms in the chains and to the Sn atoms in the square sheets presents difficulty because the compounds are metallic; this is consistent with model band structure calculations as well.[3a] Nonetheless, by drawing a parallel between the bonding in this system and the subtleties in the bonding in idealized isolated chains and sheets (above), it could be suggested that since *s-p* mixing decreases down the group,[31,32] hypervalent bonding will be more favorable for the heavier atom, Sn in this case. For the lighter Ge, s−p mixing will be significantly stronger compared to Sn and hypervalency will be less favored, suggesting that Ge-square nets would be prone to undergo Peierls distortion and break into chains.[3a] Therefore, we can speculate that Sn will be more likely to form the square-nets, whereas Ge will prefer forming the zigzag chains. Such arguments are consistent with the discussed "order" of Sn and Ge on distinct crystallographic sites, but seemingly contradicts the fact that in rare cases, such as in $TmGe_2$ and $LuGe_2$, analogous Ge-sheets do exist.[33] In these cases, however, there must be additional interactions between the square nets and the zigzag chains, which stabilize the structure by diminishing the effects of the antibonding states, as suggested by Hoffmann.[3a,34] This result will be noticeable only if the metal cations that separate the chains and the layers are small, such as Sc^{3+}, Zr^{4+}, Tm^{3+}, Lu^{3+}, Th^{4+}, U^{4+}, thereby allowing the polyanionic slabs to come closer together. An added benefit of this reasoning is that it can also explain the geometric criteria for stability of the $ZrSi_2$ type, discussed previously.

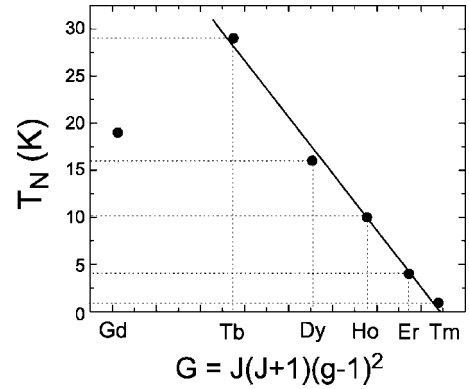

Figure 5. Néel temperatures (T_N) of RESnGe compounds (RE = Gd−Tm) plotted as a function of the corresponding rare-earth metal de Gennes factors.

Now, that we have explained the site preferences and rationalized the bonding, we can turn the attention to the systematic trends of the observed properties. The results gathered from the magnetic susceptibility measurements (Figure 2) are in excellent agreement with those expected from the de Gennes factor ($G = J(J + 1)(g_J - 1)^2$; Figure 5),[24] which is consistent with strong RKKY interactions leading to antiferromagnetic order at low temperature. The rare-earth cations are separated by ca. 3.6–3.8 Å and are too far apart for direct exchange mechanisms.[24] As evident from the plot, the decrease in the Néel temperatures for the Tb through Tm compounds follows the projected behavior. For TmSnGe, it should be noted that dc magnetization measurements showed no ordering down to 5 K, the lowest temperature measured; however, the de Gennes theory predicted that TmSnGe should have an ordering temperature below 1 K. Indeed, as shown in Figure 3, specific heat measurements provide evidence for a possible magnetic order ca. 0.9 K, although the broadness of the peak, can not completely rule out the possibility that the anomaly in $C_p(T)$ is due to short-range correlations instead of a true long-range order.

Another point regarding the magnetism among these six new lanthanide compounds, which deserves a special mention, is the fact that the Néel temperature in GdSnGe deviates from the de Gennes scaling. The reason for such a large departure from the line (Figure 5) is unclear. It could be attributed to a breakdown of the de Gennes scaling due to the slightly higher Sn content in GdSnGe, thereby to an off-scale increase in the unit cell volume (Table 2) or change in the electronic density of states. Another possible explanation involves an admixture of close in energy states for the Gd^{3+} ion, which arise from splitting of the spin-only multiplet due to crystalline field effects and/or electronic correlations (e.g., $^6P_{5/2}$ and $^8S_{7/2}$). Similar deviations for series of isostructural germanides and stannides can be recognized for $RECo_xGe_2$ and $RECo_xSn_2$ (RE = Gd−Er) with the $CeNiSi_2$ and $CeNiSn_2$-types, respectively.[35]

We also note that for GdSnGe, the specific heat curve shows not a single, but two broad anomalies (Figure 3). The first is observed at ca. 20 K and is consistent with the antiferromagnetic

(32) Ienco, A.; Hoffmann, R.; Papoian, G. *J. Am. Chem. Soc.* **2001**, *123*, 2317.

(33) Extended structures with isolated (i.e., analogous to those in $TmGe_2$) square nets of Si and Ge are very rare. Such motifs can be stabilized by many ways, through capping by transition metals for example. This is exemplified by the compounds adopting the $CeNiSi_2$ type, the bonding in which is usually described in terms of $NiSi_4$ square pyramids fused in their bases in a manner reminiscent of the topology of the PbO-type.[15] The transition metal is shown to have significant interactions with the square sheets.

(34) Albert, K.; Meyer, H.-J.; Hoffmann, R. *J. Solid State Chem.* **1993**, *106*, 201.

(35) (a) Baran, S.; Henkel, F.; Kaczorowski, D.; Hernández-Velasco, J.; Penc, B.; Stüßer, N.; Szytula, A.; Wawrzynska, E. *J. Alloys Compd.* **2006**, *415*, 1. (b) Gil, A.; Penc, B.; Wawrzynska, E.; Hernández-Velasco, J.; Szytula, A.; Zygmunt, A. *J. Alloys Compd.* **2004**, *365*, 31.

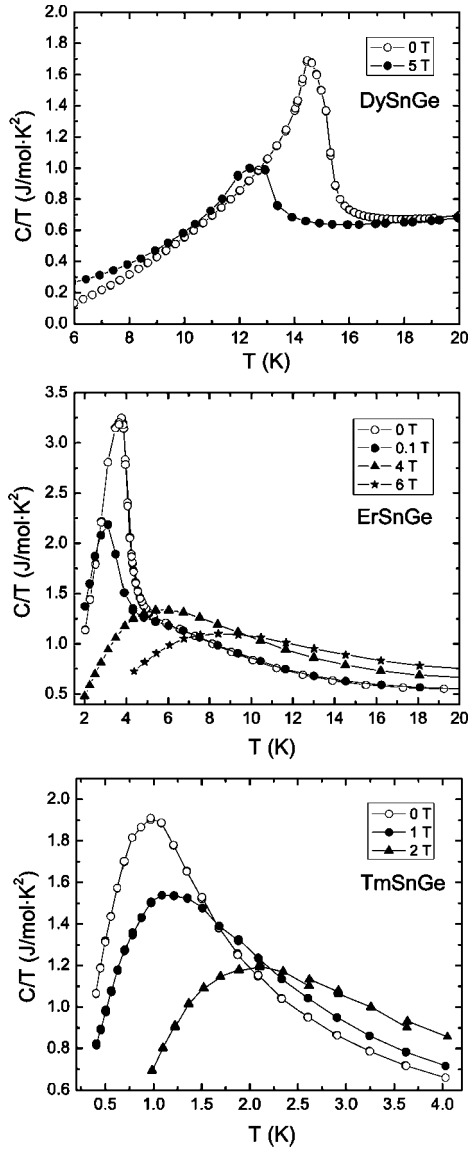

Figure 6. Field-dependent specific heat for RESnGe (RE = Dy, Er, Tm).

ordering as determined by the magnetization; the second anomaly is clearly seen at *ca.* 5 K. Since $\chi(T)$ and $\rho(T)$ plots do not corroborate the hypothesis for a subsequent magnetic order, the peak at 5 K most certainly can be attributed to a spin-reorientation. A similar spin reorientation may also exist in TbSnGe.

At temperatures below 10 K, the specific heat data for GdSnGe can be seen as not approaching to zero as its isostructural analogues do, rather, the electronic specific heat coefficient γ ($= C_P/T$) is on the order of 150 mJ/mol K^2. It is indeed large but cannot be attributed to a heavy fermion behavior though as the corresponding T^2 term in resistivity is not observed. The fact that the specific heat is rising slightly at the lowest temperatures suggests it may originate from nuclear Schottky effects,[24] although it is peculiar that similar upturns are not observed in any of the other compounds.

Selected field-dependent specific heat measurements were carried out and the results are displayed in Figure 6. In the Dy and Er compounds, the entropy released is roughly R ln(2), consistent with a doublet ground state.[24] The applied magnetic field initially suppresses the transition, as expected for antiferromagnetically ordered systems. However, for ErSnGe, larger fields reveal a broad peak that increases in temperature with increasing fields. This may be expected due to the Zeeman splitting of the ground-state doublet. Indeed, the energy scale of the peak position corresponds roughly to $g\mu_B H$. For DySnGe, we did not reach large enough fields, where we would expect to start observing this behavior. In the case of TmSnGe, where the broad peak in zero field may be reflecting short-range correlations as opposed to long-range order, the small energy scale of the correlated behavior (0.9 K) is easily overcome with magnetic fields as small as 10 kOe where the peak clearly shifts to higher temperatures with increasing field, again consistent with simple Zeeman splitting arguments.

Conclusions

Seven new ternary compounds $RESn_{1+x}Ge_{1-x}$ (RE = Y, Gd−Tm; $x \approx \pm 0.15$) have been synthesized and structurally characterized by single-crystal X-ray diffraction. They crystallize with the orthorhombic space group *Cmcm* and can be viewed as nearly ordered ternary variants of the $ZrSi_2$ type,[15] obtained by "coloring" the anionic sites with two different elements, Ge and Sn. Within this explanation, the $RESn_{1+x}Ge_{1-x}$ structures present rare examples of site preferences between two tetrel elements, which is related to the tendency of the heavier *p*-block elements to favor hypervalent bonding arrangements. Magnetic susceptibility and calorimetry measurements show that these compounds, excluding YSnGe order antiferromagnetically at low temperatures. The Néel temperatures for all, with an exception of GdSnGe, are in excellent agreement with those expected from the de Gennes factor and indicate strong RKKY interactions. The expected metallic properties are confirmed from temperature-dependent resistivity measurements.

The ability of the structure to adapt to subtle "coloring" changes makes it suitable for further case studies via doping with other elements. In light of the discussion presented herein, we speculate that introducing extra electrons into the system, for instance, by virtue of replacing Sn with Sb (assuming Sb will form the nets), would result in optimal valence electron concentration and stabilize the square network without the need for distortion. Such studies are currently underway.

Acknowledgment. S.B. acknowledges financial support from the University of Delaware. P.H.T. thanks the International Centre for Diffraction Data (ICDD) for the 2007 Ludo Frevel Crystallographic Fellowship. Work at LANL is done under the auspices of the U.S. DOE.

Supporting Information Available: A combined X-ray crystallographic file in CIF format (all compounds); refined unit cell dimensions from bulk powder samples, along with plots of the actual powder patterns, tables with atomic coordinates and equivalent displacement parameters, important bond distances for RESnGe (RE = Y, Gd−Er), plots of the coordination polyhedra of the rare-earth metal cations, magnetic susceptibility vs T for $TmGe_2$ and YSnGe, specific heat of YSnGe vs T; magnetic entropy vs T for all RESnGe (RE = Gd, Tm) (PDF). This material is available free of charge via the Internet at http://pubs.acs.org.

CM7033799